Optická emisní spektroskopie atomů

Diagnostické metody 1

Zdeněk Navrátil

Ústav fyzikální elektroniky Přírodovědecké fakulty Masarykovy univerzity, Brno

Outline

Instrumentation

- typically grating spectrometer of Czerny-Turner mounting equipped with CCD/ICCD detector
- spectral range and sensitivity: detector (silicon CCD, photocathode), grating efficiency
- resolution: number of illuminated grating grooves, slit width, pixel size

$$R = \lambda/\Delta\lambda = mN$$

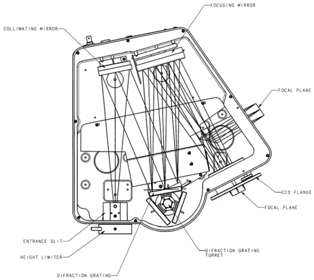

Technique overview – how we measure

- collecting the light emitted by plasma (optical emission spectroscopy, OES):
  - non-intrusive
  - sensing the light at the plasma boundary
  - optical probes
- sending the light through the plasma (optical absorption spectroscopy):
  - based on Lambert-Beer law
  - can disturb the plasma, two ports
  - white light, hollow cathode lamps, LASERS DM2 – Dvořák
- collecting the light emitted and reabsorbed by the plasma (self-absorption methods of OES)

Technique overview – how we measure

- collecting the light emitted by plasma (optical emission spectroscopy, OES):
  - non-intrusive
  - sensing the light at the plasma boundary → self-absorption can play a role
  - optical probes
- sending the light through the plasma (optical absorption spectroscopy):
  - based on Lambert-Beer law
  - can disturb the plasma, two ports
  - white light, hollow cathode lamps, LASERS DM2 – Dvořák
- collecting the light emitted and reabsorbed by the plasma (self-absorption methods of OES)

Technique overview – what we look at

- line positions (wavelengths): electric, magnetic fields, atom velocities (Stark, Zeeman, Doppler effect)
- lineshapes and linewidths: electron density, gas pressure, density, temperatures (Stark, van der Waals, resonance, Doppler line broadening) DM1 – Synek
- line intensities: . . . all

Technique overview – what we look at

- line positions (wavelengths): electric, magnetic fields, atom velocities (Stark, Zeeman, Doppler effect)
- lineshapes and linewidths: electron density, gas pressure, density, temperatures (Stark, van der Waals, resonance, Doppler line broadening) DM1 – Synek
- line intensities: . . . all
  - relative – instrument spectral sensitivity is taken into account, no absolute intensity calibration is performed
    output: relative populations of excited states, excitation temperatures etc.
  - absolute – access to absolute densities of excited states, electron density etc.

Absolute intensity measurement

- radiant flux/zářivý tok – energy emitted/incident on surface per unit time

$$\Phi = \frac{\mathrm{d}\mathscr{E}}{\mathrm{d}t}, \quad \mathrm{W} \tag{1}$$

- irradiance – flux density (per unit surface)

$$I = \frac{\mathrm{d}\Phi}{\mathrm{d}S} = \frac{\mathrm{d}^2\mathscr{E}}{\mathrm{d}t\mathrm{d}S}, \quad \mathrm{W\,m^{-2}} \tag{2}$$

  - specified during calibratrion of calibrated light sources (spectral irradiance)
  - optical fibre is not a detector of irradiance (acceptance angle)
  - radiometric irradiance probes, cosine correction diffusers, integrating spheres, . . .

Absolute intensity measurement 2

- radiance (zář) – radiant flux per unit perpendicular surface and unit solid angle

$$L = \frac{\mathrm{d}^2\Phi}{\mathrm{d}S\cos\theta\,\mathrm{d}\Omega} = \frac{\mathrm{d}^3\mathscr{E}}{\mathrm{d}t\,\mathrm{d}S\cos\theta\,\mathrm{d}\Omega}, \quad \mathrm{W\,m^{-2}\,sr^{-1}} \qquad (3)$$

- radiance × irradiance

$$I = \int_\Omega L(\theta)\cos\theta\,\mathrm{d}\Omega \qquad (4)$$

For constant L (Lambert) radiators $I = \pi L$.

- for description of radiating solid surfaces

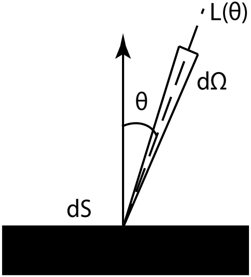

Absolute intensity measurement 3

- emission coefficient – radiant power emited by unit volume into unit solid angle

$$j = \frac{\mathrm{d}^3 \mathscr{E}}{\mathrm{d}t\,\mathrm{d}V\,\mathrm{d}\Omega}. \qquad (5)$$

- all quantities have their spectral densities, e.g. $j(\lambda)$

emission coefficient of transition

$$j_{ij} = \frac{1}{4\pi} n_i A_{ij} h\nu_{ij}$$

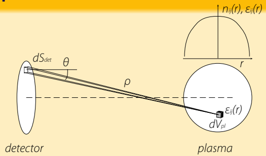

$$I_{ij} = \frac{1}{S_{\mathrm{det}}} \int_{V_{\mathrm{pl}}} \int_{S_{\mathrm{det}}} \frac{j_{ij}(r)}{\rho^2} \mathrm{Acc}(\theta) \mathrm{d}V_{\mathrm{pl}} \mathrm{d}S_{\mathrm{det}}$$

irradation of detector for optical thin plasma condition

Electron temperature from Boltzmann plot?

- density of atoms in excited state

$$n_i = n \frac{g_i}{Q} \mathrm{e}^{-\frac{\mathscr{E}_i}{k_\mathrm{b} T_\mathrm{e}}} \quad (6)$$

g_i – statistical weight, $\mathscr{E}_i$ – excitation energy, n – atom density, Q – state sum, T_e excitation temperature (= electron temperature)

- spectral line intensity

$$I \propto n_i A_{ij} \frac{hc}{\lambda} \quad (7)$$

$$I = C \cdot \frac{g_i A_{ij}}{\lambda} \mathrm{e}^{-\frac{\mathscr{E}_i}{k_\mathrm{b} T_\mathrm{e}}} \quad (8)$$

- Boltzmann plot

$$\ln \frac{I\lambda}{g_i A_{ij}} = -\frac{1}{k_\mathrm{b} T_\mathrm{e}} \mathscr{E}_i + \ln k_1, \quad (9)$$

Possibilities for excitation temperature measurement

excited level balance

- local thermodynamic equilibrium (LTE) plasma
  - LTE condition

$$n_e \gg 1.6 \cdot 10^{12} \sqrt{T_e} (\Delta E)^3 \quad (\mathrm{cm}^{-3})$$

  - electron temperature from Boltzmann plot
- non-LTE plasma
  - corona equilibrium, excitation saturation phase, . . .
  - low electron density plasma
  - use of Boltzmann-plot leads to erroneous electron temperature
  - CR modelling

non-Maxwellian EDF

- inelastic collisions, beam electrons, non-local EDF

Quasi-steady state-solution of differential equations

coupled DE for densities of excited states

$$\frac{\partial n_i}{\partial t} + \nabla(n_i \vec{v}) = \left(\frac{\partial n_i}{\partial t}\right)_{\mathrm{c,r}} \tag{10}$$

population and depopulation processes are very fast:

$$\frac{\partial n_i}{\partial t} = \left(\frac{\partial n_i}{\partial t}\right)_{\mathrm{c,r}} = 0 \tag{11}$$

not valid for ground-state atoms, ions, metastables, high pressure

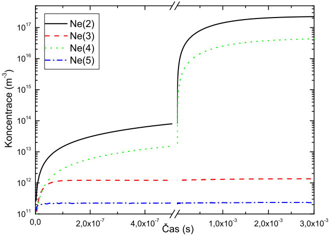

Level balance

$$\frac{\partial n_0}{\partial t} + \bigtriangledown(n_0 \vec{v_0}) = -S_{\mathrm{cr}} n_{\mathrm{e}} n_0 + \alpha_{\mathrm{cr}} n_{\mathrm{e}} n_{\mathrm{ion}}$$

$$\frac{\partial n_{\mathrm{ion}}}{\partial t} + \bigtriangledown(n_{\mathrm{ion}} \vec{v_{\mathrm{ion}}}) = +S_{\mathrm{cr}} n_{\mathrm{e}} n_0 - \alpha_{\mathrm{cr}} n_{\mathrm{e}} n_{\mathrm{ion}}$$

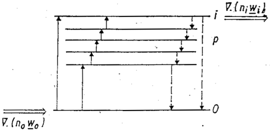

ionizing plasma

classification of models (plasma state)

- ionizing plasma $S_{\mathrm{cr}} n_{\mathrm{e}} n_0 - \alpha_{\mathrm{cr}} n_{\mathrm{e}} n_{\mathrm{ion}} > 0$
  - plasma conducting current, ionizing waves
- recombining plasma $S_{\mathrm{cr}} n_{\mathrm{e}} n_0 - \alpha_{\mathrm{cr}} n_{\mathrm{e}} n_{\mathrm{ion}} < 0$
  - afterglows, outer regions of flames
- equilibrium plasma $S_{\mathrm{cr}} n_{\mathrm{e}} n_0 - \alpha_{\mathrm{cr}} n_{\mathrm{e}} n_{\mathrm{ion}} = 0$ (ioniozation-recombination equilibrium)

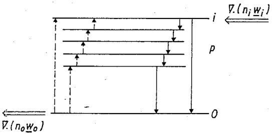

recombining plasma

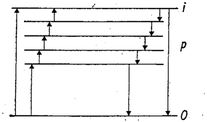

equilibrium plasma

Excitation phases: corona phase

population by electron impact excitation, radiative deexcitation

$$k_{0i}^{\mathrm{el}} n_{\mathrm{e}} n_0 + k_{\mathrm{m}i}^{\mathrm{el}} n_{\mathrm{e}} n_{\mathrm{m}} (+ \sum_{j>i} \Lambda_{ji} A_{ji} n_j) = \sum_{j<i} \Lambda_{ij} A_{ij} n_i \tag{12}$$

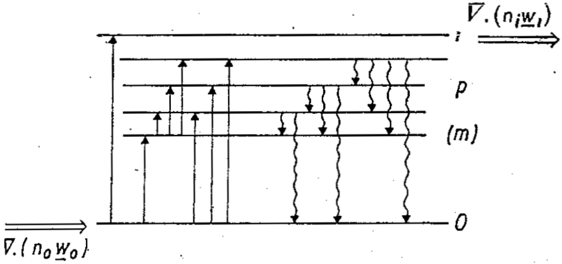

Excitation phases: excitation saturation phase

population and depopulation by electron impact

$$\sum_{j \neq i} k_{ji}^{\mathrm{el}} n_{\mathrm{e}} n_j + (\alpha_i n_{\mathrm{e}} n_{\mathrm{ion}}) = \sum_{j \neq i} k_{ij}^{\mathrm{el}} n_{\mathrm{e}} n_i + S_i n_{\mathrm{e}} n_i$$

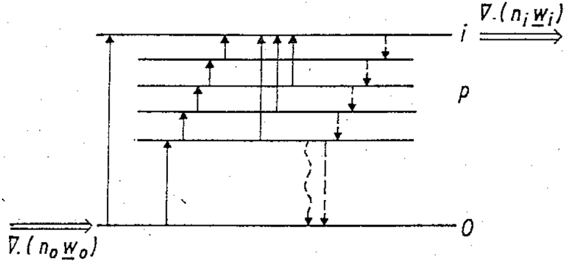

- saturation of the excited state densities with increasing n_{e}
- no Saha equilibrium, $S_i n_i \gg \alpha_i n_{\mathrm{ion}}$

Excitation phases: excitation saturation phase 2

- stepwise excitation → ladder-like excitation flow

$$k_{i-1,i} n_{\mathrm{e}} n_{i-1} - k_{i,i-1} n_{\mathrm{e}} n_i = k_{i,i+1} n_{\mathrm{e}} n_i - k_{i+1,i} n_{\mathrm{e}} n_{i+1} - S_i n_{\mathrm{e}} n_i$$

Excitation phases: partial local thermodynamic equilibrium

- 2 equilibria: excited state $\times$ ion state, neighbouring excited states
- ionization $\sim$ recombination $\gg$ excitation flow

$$k_{i-1,i} n_\mathrm{e} n_{i-1} - k_{i,i-1} n_\mathrm{e} n_i = k_{i,i+1} n_\mathrm{e} n_i - k_{i+1,i} n_\mathrm{e} n_{i+1} - S_i n_\mathrm{e} n_i + \alpha_i n_\mathrm{e} n_\mathrm{ion}$$

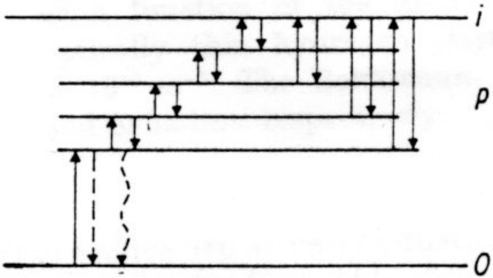

Role of collisional processes

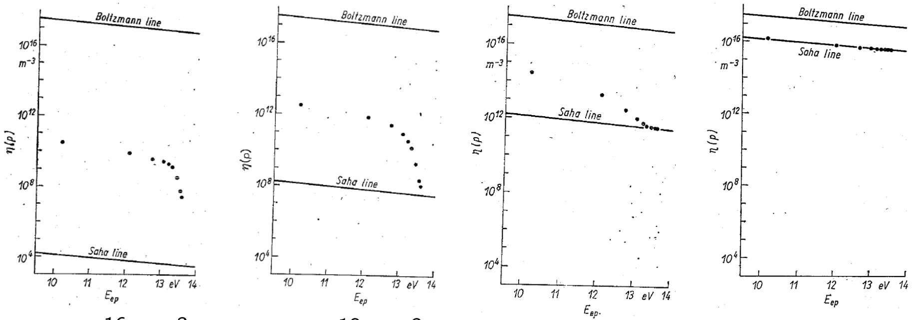

$n_e = 10^{16}$ m^{-3} $\quad$ $n_e = 10^{18}$ m^{-3} $\quad$ $n_e = 10^{20}$ m^{-3} $\quad$ $n_e = 10^{22}$ m^{-3}

Boltzmann	$n_i^B = n_0 g_i / g_0 e^{-E_i/kT_e}$
Saha	$n_i^S = n_e n_{ion} \frac{g_i}{g_e g_{ion}} (h^2/2\pi m_e k T_e)^{3/2} e^{E_{ion,i}/kT_e}$
deviation from B & S	$n_i = r_i^0 n_i^S + r_i^1 n_i^B$

Excitation phases

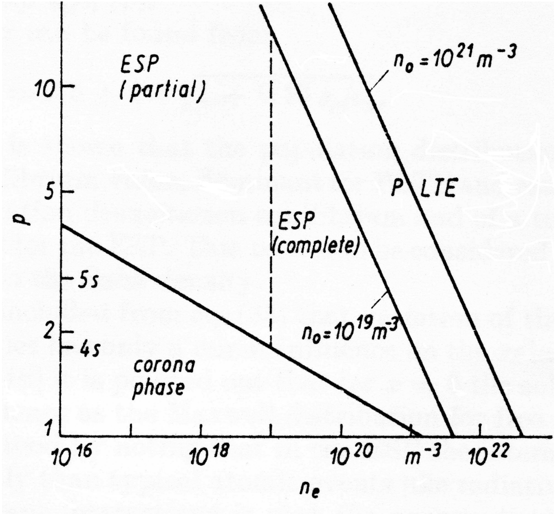

Collisional-radiative model

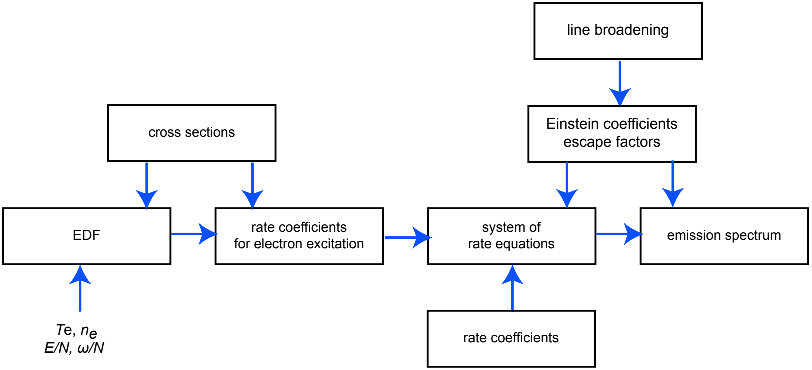

Electron distribution function

- Maxwellian EDF
- solution of Boltzmann kinetic equation
- normalization of the EDF

$$\int_0^\infty f(\varepsilon)\varepsilon^{1/2}\mathrm{d}\varepsilon = 1 \tag{13}$$

- mean electron energy

$$\langle\varepsilon\rangle = \int_0^\infty f(\varepsilon)\varepsilon^{3/2}\mathrm{d}\varepsilon, \tag{14}$$

- rate coefficients k, $k_{\rm inv}$ of electron collision with cross section σ and of inverse process

$$k = \sqrt{\frac{2e}{m_{\rm e}}}\int_0^\infty \sigma(\varepsilon)f_0(\varepsilon)\varepsilon\mathrm{d}\varepsilon$$

$$k_{\rm inv} = \sqrt{\frac{2e}{m_{\rm e}}\frac{g_j}{g_i}}\int_{\varepsilon_{ij}}^\infty \sigma(\varepsilon)f_0(\varepsilon-\varepsilon_{ij})\varepsilon\mathrm{d}\varepsilon$$

Approaches of OES data processing

- line ratio methods
  - selection of convenient line pair (sensitivity, model simplicity, ease of measurement)
  - no control of model validity
- „many line fitting“methods

Electron temperature and EDF measurement by OES+CR

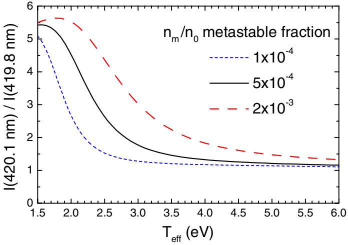

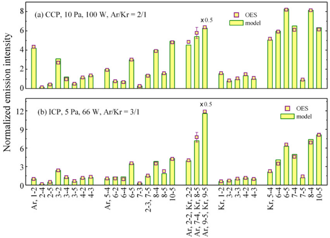

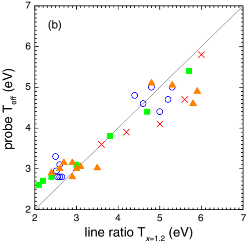

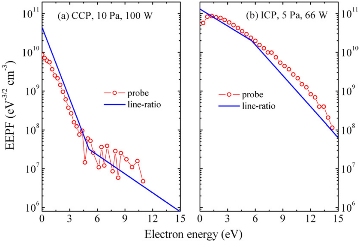

Boffard J B *et al* 2012 *J. Phys. D: Appl. Phys.* **45** 045201

Zhu X-M *et al* 2012 *Plasma Sources Sci. Technol.* **21** 024003

TRG spectroscopy

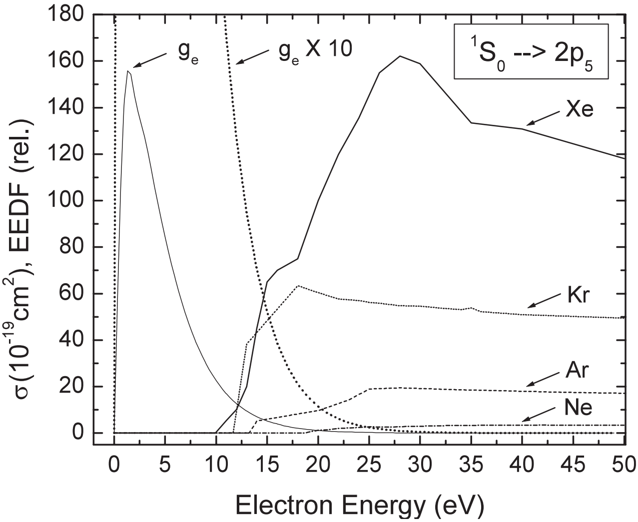

Electric field measurement

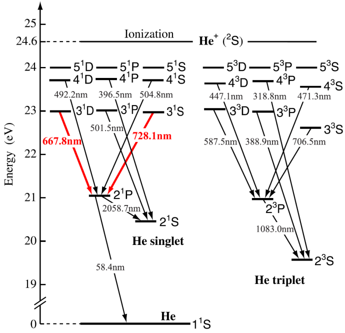

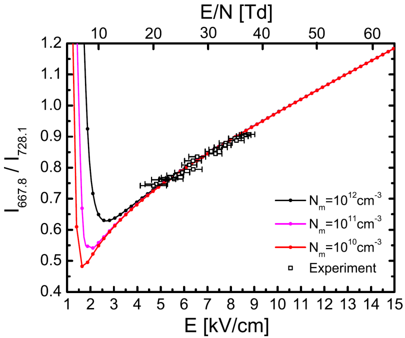

Ivkovic S S *et al* 2014 *J. Phys. D: Appl. Phys.* **47** 055204

Excited levels

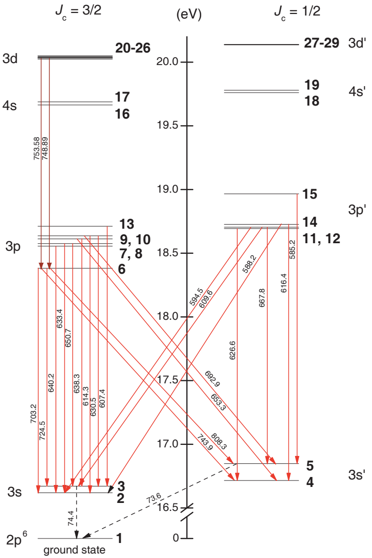

i	*nlpqr*	Racah	Paschen		(eV)
1	21000	$2p^6$	$1p_0$	1	0.000000
2	30332	$3s\ [3/2]^o_2$	$1s_5$	5	16.61907
3	30331	$3s\ [3/2]^o_1$	$1s_4$	3	16.67083
4	30110	$3s'\ [1/2]^o_0$	$1s_3$	1	16.71538
5	30111	$3s'\ [1/2]^o_1$	$1s_2$	3	16.84805
6	31311	$3p\ [1/2]_1$	$2p_{10}$	3	18.38162
7	31353	$3p\ [5/2]_3$	$2p_9$	7	18.55511
8	31352	$3p\ [5/2]_2$	$2p_8$	5	18.57584
9	31331	$3p\ [3/2]_1$	$2p_7$	3	18.61271
10	31332	$3p\ [3/2]_2$	$2p_6$	5	18.63679
11	31131	$3p'\ [3/2]_1$	$2p_5$	3	18.69336
12	31132	$3p'\ [3/2]_2$	$2p_4$	5	18.70407
13	31310	$3p\ [1/2]_0$	$2p_3$	1	18.71138
14	31111	$3p'\ [1/2]_1$	$2p_2$	3	18.72638
15	31110	$3p'\ [1/2]_0$	$2p_1$	1	18.96596
16	40332	$4s\ [3/2]^o_2$	$2s_5$	5	19.66403
17	40331	$4s\ [3/2]^o_1$	$2s_4$	3	19.68820
18	40110	$4s'\ [1/2]^o_0$	$2s_3$	1	19.76060
19	40111	$4s'\ [1/2]^o_1$	$2s_2$	3	19.77977
20	32310	$3d\ [1/2]^o_0$	$3d_6$	1	20.02464
21	32311	$3d\ [1/2]^o_1$	$3d_5$	5	20.02645
22	32374	$3d\ [7/2]^o_4$	$3d'_4$	9	20.03465
23	32373	$3d\ [7/2]^o_3$	$3d_4$	7	20.03487
24	32332	$3d\ [3/2]^o_2$	$3d_3$	5	20.03675
25	32331	$3d\ [3/2]^o_1$	$3d_2$	3	20.04039
26	32352	$3d\ [5/2]^o_2$	$3d''_1$	5	20.04821
	32353	$3d\ [5/2]^o_3$	$3d'_1$	7	20.04843
27	32152	$3d'\ [5/2]^o_2$	$3s''''_1$	5	20.13611
	32153	$3d'\ [5/2]^o_3$	$3s'''_1$	7	20.13630
28	32132	$3d'\ [3/2]^o_2$	$3s''_1$	5	20.13751
29	32131	$3d'\ [3/2]^o_1$	$3s'_1$	3	20.13946

Considered elementary processes

1. Electron impact excitation out of the g.s.

$$\mathrm{Ne}(1) + \mathrm{e}^- \xrightarrow{k_{1j}} \mathrm{Ne}(j) + \mathrm{e}^-, \quad j = 2, \ldots 29$$

2. Electron impact excitation out of $2p^5 3s$ states

$$\mathrm{Ne}(i) + \mathrm{e}^- \xrightarrow{k_{ij}} \mathrm{Ne}(j) + \mathrm{e}^-, \quad i = 2, \ldots 5,\ j = 6, \ldots 15$$

3. Electron impact deexcitation to the g.s. and $2p^5 3s$ states

$$\mathrm{Ne}(i) + \mathrm{e}^- \xrightarrow{k_{ij}} \mathrm{Ne}(j) + \mathrm{e}^-, \quad i = 2, \ldots 29,\ j = 1, \ldots 5,\ i > j$$

4. Electron induced excitation transfer among $2p^5 3s$ states

$$\mathrm{Ne}(i) + \mathrm{e}^- \xrightarrow{k_{ij}} \mathrm{Ne}(j) + \mathrm{e}^-, \quad i, j = 2, \ldots 5$$

5. Spontaneous emission and absorption of radiation

$$\mathrm{Ne}(i) \xrightarrow{\Lambda_{ij} A_{ij}} \mathrm{Ne}(j) + h\nu, \quad i = 2, \ldots 29,\ i > j$$

Considered elementary processes 2

6. Two-body collision induced deactivation and excitation transfer among $2p^53p$ states

$$\mathrm{Ne}(i) + \mathrm{Ne}(1) \xrightarrow{k_{ij}} \mathrm{Ne}(j) + \mathrm{Ne}(1), \quad i,j = 6,\ldots 15$$

7. Chemoionization

$$\mathrm{Ne}(2-5) + \mathrm{Ne}(2-5) \xrightarrow{k_{\mathrm{met}}} \mathrm{Ne}(1) + \mathrm{Ne}^+ + \mathrm{e}^-$$

8. Two-body collision induced deactivation

$$\mathrm{Ne}(2-5) + \mathrm{Ne}(1) \xrightarrow{k_{2b}} 2\mathrm{Ne}(1)$$

9. Penning ionization of impurities

$$\mathrm{Ne(2\text{-}5)} + \mathrm{H_2} \xrightarrow{k_{\mathrm{H_2}^+}} \mathrm{H_2}^+ + \mathrm{Ne}(1) + \mathrm{e}^-$$

$$\mathrm{Ne(2\text{-}5)} + \mathrm{H_2} \xrightarrow{k_{\mathrm{NeH}^+}} \mathrm{NeH}^+ + \mathrm{H} + \mathrm{e}^-$$

$$\mathrm{Ne(2\text{-}5)} + \mathrm{N_2} \xrightarrow{k_{\mathrm{N_2}^+}} \mathrm{N_2}^+ + \mathrm{Ne}(1) + \mathrm{e}^-$$

Considered elementary processes 3

12. Electron impact ionization of the ground-state and metastable atoms
13. Three-body production of dimers

$$\mathrm{Ne}(2,4)+\mathrm{Ne}(1)+\mathrm{Ne}(1) \stackrel{k_{3\mathrm{b_m}}}{\rightarrow} \mathrm{Ne}_2^*+\mathrm{Ne}(1)$$

$$\mathrm{Ne}(3)+\mathrm{Ne}(1)+\mathrm{Ne}(1) \stackrel{k_{3\mathrm{b_3}}}{\rightarrow} \mathrm{Ne}_2^{\mathrm{m}}+\mathrm{Ne}(1)$$

$$\mathrm{Ne}(5)+\mathrm{Ne}(1)+\mathrm{Ne}(1) \stackrel{k_{3\mathrm{b_5}}}{\rightarrow} \mathrm{Ne}_2^{\mathrm{m}}+\mathrm{Ne}(1)$$

Spontaneous emission

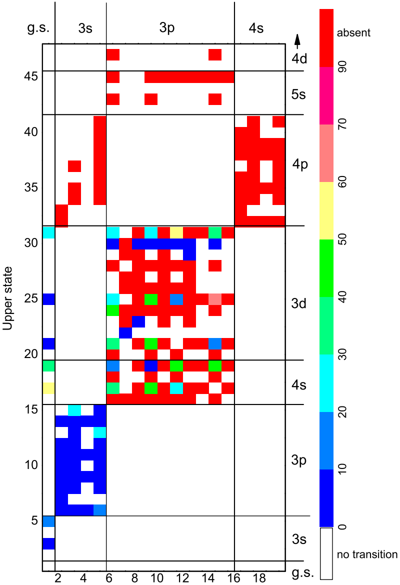

Einstein coefficient A_{ij}

$$A_{ij} = \frac{16\pi^3\nu^3}{3\varepsilon_0 hc^3}\frac{S}{g_i}$$

$$A_{ij} = \frac{g_j}{g_i}\frac{2\pi e^2\nu^2}{\varepsilon_0 mc^3}f$$

effective levels

$$A_{\{i\}j} = \frac{\sum_i g_i A_{ij}}{\sum_i g_i}$$

$\leftarrow$ relative differences of two data source – NIST and Seaton 1998

Absorption of radiation

Number of absorption transitions between states i, j (j is lower) in unit volume is

$$n_j B_{ji} \rho(\omega_0)$$

What is $\rho(\omega_0)$?

The spatial distribution of population of excited state due to the radiation propagation can be described by Holstein equation

$$\frac{\partial n(\vec{r})}{\partial t} = -An(\vec{r}) + A \int n(\vec{r}') G(\vec{r}', \vec{r}) \mathrm{d}\vec{r}', \qquad (15)$$

$$G(\vec{r}', \vec{r}) = -\frac{1}{4\pi\rho^2} \frac{\partial T}{\partial \rho}, \rho = |\vec{r}' - \vec{r}|, \quad T(\rho) = \int f(\omega) \mathrm{e}^{-kf(\omega)\rho} \mathrm{d}\omega.$$

Solution of Holstein equation has a form

$$n(\vec{r}, t) = \sum_j c_j n_j(\vec{r}) \mathrm{e}^{-A/g_j t}, \qquad (16)$$

in which g_j are *trapping* factors attached to eigenfunctions n_j.

Escape factor $\Lambda = 1/g_0$.

Trapping factor

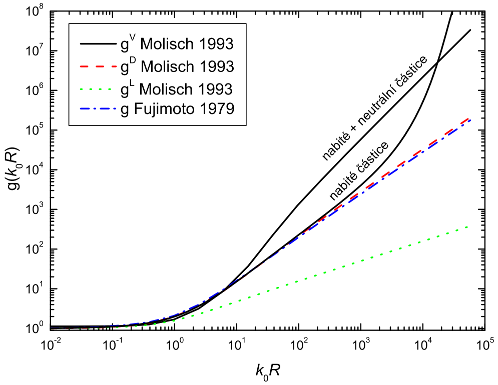

Parameters of solution:

- discharge geometry
- opacity $k_0 R$
- spectral line profile

Solution of rate-equations

Initial conditions

$$n_i(t=0) = \begin{cases} N \equiv \frac{p}{k_\mathrm{b} T_\mathrm{n}}, & i = 1 \\ 0, & i > 1 \end{cases} \tag{17}$$

- Runge-Kutta methods
- stationary state solution: all excited states reach stationary state ($\frac{\partial n_i}{\partial t} = 0$)
- Non-linear dependence of some rate equations

$$\left(\frac{\partial n_2}{\partial t}\right)_\mathrm{met} = -4k_\mathrm{met} n_2^2 - 2k_\mathrm{met} n_2 n_4 - \ldots - (k_{\mathrm{H_2}^+} + k_{\mathrm{NeH}^+})[\mathrm{H_2}]n_2 - -(k_{\mathrm{N_2}^+} + k_{\mathrm{NeN_2}^+})[\mathrm{N_2}]n_2 - k_{\mathrm{O_2}^+}[\mathrm{O_2}]n_2 - \frac{D_2}{l_\mathrm{D}^2} n_2 - k_\mathrm{ionmet} n_\mathrm{e} n_2$$

Spectrum calculation and comparison

- measured spectral line intensities, integrated over lineshapes

  $[\lambda_k, I_k^{\mathrm{exp}}],\ k = 1, \ldots n,\ n = 30$

- calculated total emission coefficients of transitions

  $$I_{ij}^{\mathrm{cr}} = \frac{1}{4\pi} n_i \Lambda_{ij} A_{ij} h\nu_{ij}$$

- comparison of spectra by least squares method

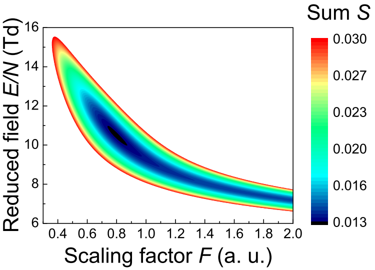

$$\mathscr{S} = \sum_{k=1}^{n} \frac{(\mathscr{F} \cdot I_k^{\mathrm{cr}}(T_e, n_e, n_{1\mathrm{s}_3}, n_{1\mathrm{s}_5}) - I_k^{\mathrm{exp}})^2}{I_k^{\mathrm{exp}}}$$

Role of metastables

- simplified 0D scheme is not valid

$$\frac{\partial n_i}{\partial t} + \nabla(n_i \vec{v}) = \left(\frac{\partial n_i}{\partial t}\right)_{\mathrm{c,r}} \quad (18)$$

- longer computational times
- increased sensitivity at low electron energies

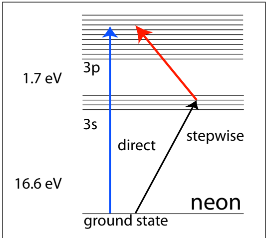

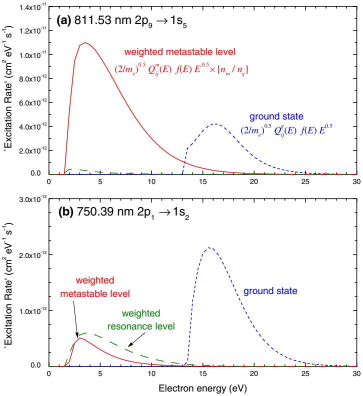

argon

Boffard J B, Jung R O, Lin C C and Wendt A E 2010 *Plasma Sources Sci. Technol.* 19(6)

Direct and stepwise excitation

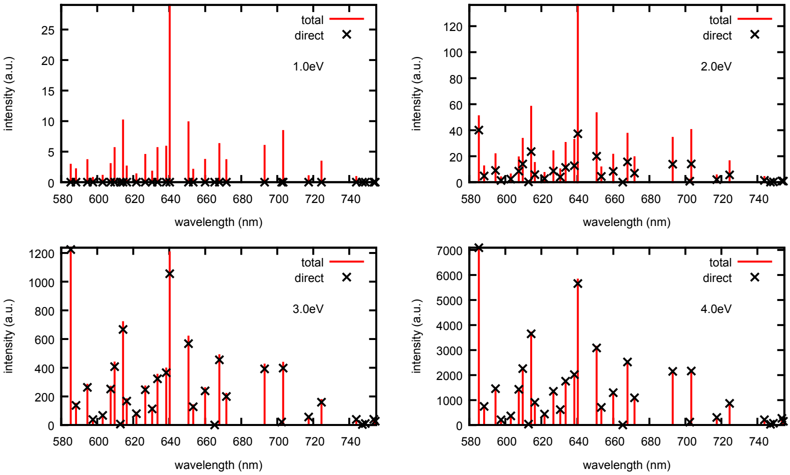

Maxwellian EDF, gas temperature 300 K, fixed densities of all $1s_i$ levels

DC glow discharge in neon

- positive column of DC glow discharge at 1.1 Torr
- OES in spectral range 300 – 850 nm
- CR model with stationary BKE solver
- probe measurement

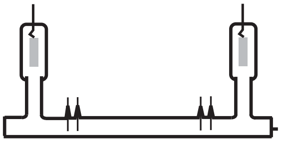

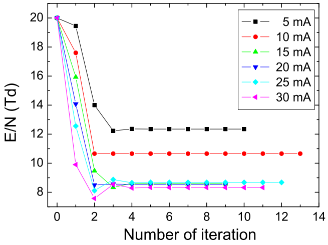

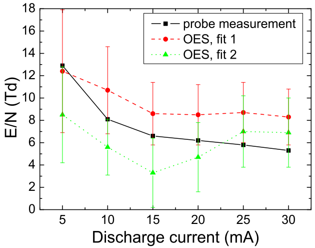

Navrátil Z, Trunec D, Hrachová V and Kaňka A 2007 *J. Phys. D: Appl. Phys.* 40(4) 1037

Radio-frequency discharge in neon

- capacitively coupled RF discharge in neon (13.56 MHz)
- low pressure (10 Pa)
- reactor R3 “Temelín”, inner diameter 33 cm, discharge gap 40 mm, electrodes 8 cm in diameter
- studied by OES/CR, OAS, PIC/MC, Langmuir probe
- absolute intensity measurement

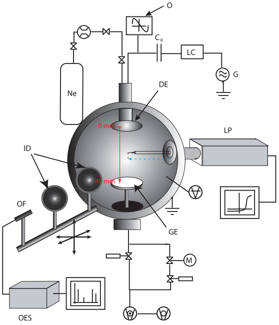

RF (13.56 MHz) capacitive discharge in neon at 10 Pa

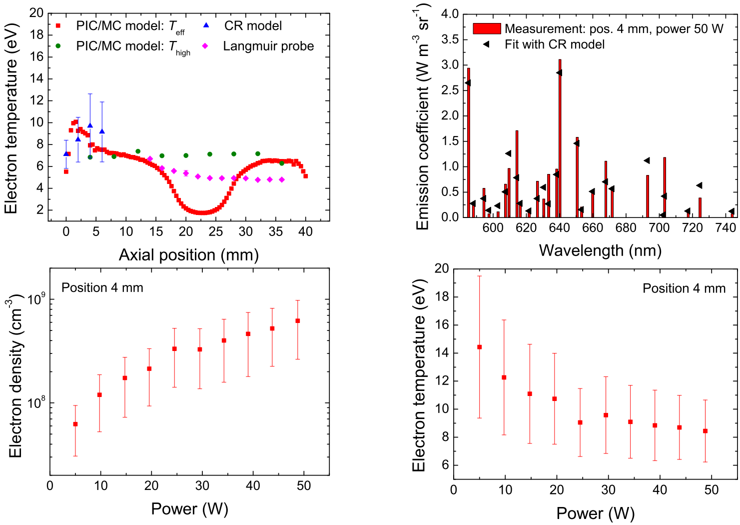

Navrátil Z, Dvořák P, Brzobohatý O and Trunec D 2010 *J. Phys. D: Appl. Phys.* **43**(50) 505203.

MW surface-wave driven discharge in neon in coaxial configuration

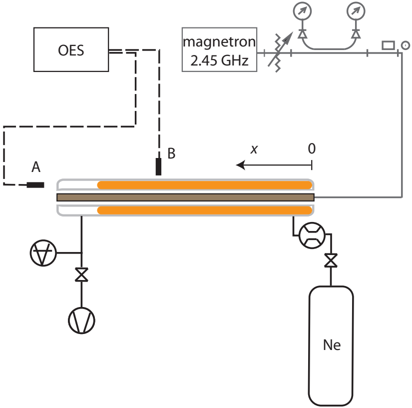

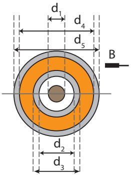

argon

- two-cylinder quartz tube with copper rod antenna, length 320 mm, dimensions $d_1 = 5$ mm, $d_2 = 7$ mm, $d_3 = 11$ mm, $d_4 = 20$ mm and $d_5 = 24$ mm
- microwave power 60 W

Electron distribution function

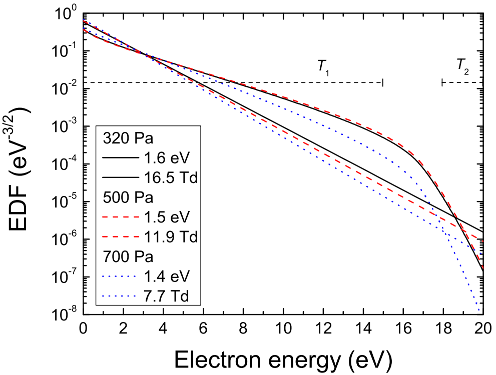

$$T_1 = 2.1 - 2.5 \text{ eV}, \qquad \mathscr{E} < 15\,\text{eV}$$
$$T_2 = 0.33 - 0.43 \text{ eV} \qquad 18\,\text{eV} < \mathscr{E} < 20\,\text{eV}$$
$$T_e = 1.4 - 1.6 \text{ eV} \qquad \text{Maxwellian}$$

Spectra fit

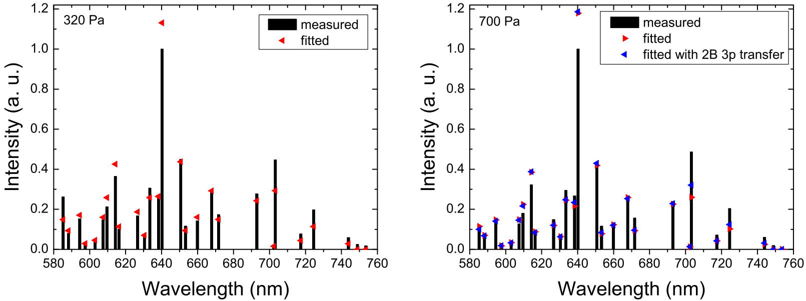

- using BKE solver
- effect of deactivation by heavy particles on spectra under studied conditions is small

Sensitivity to electron density and metastable density

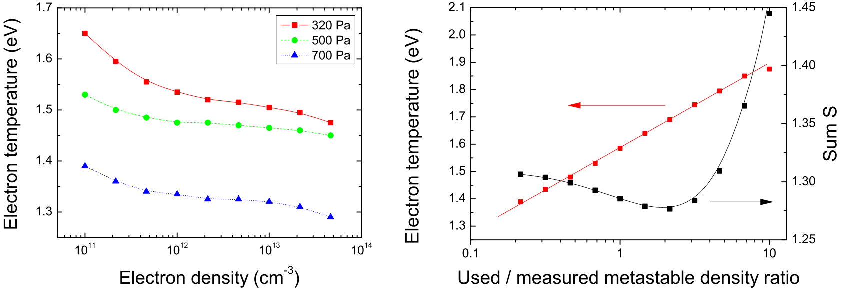

sensitivity to metastables: 0.3 eV or 2 Td per order of density

Axial dependencies for $T = 300$ K

Maxwellian EDF

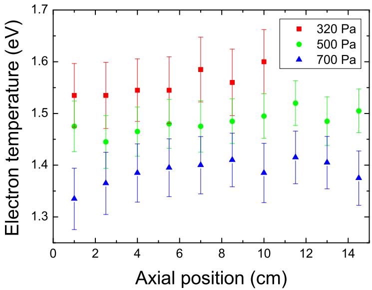

solution BKE

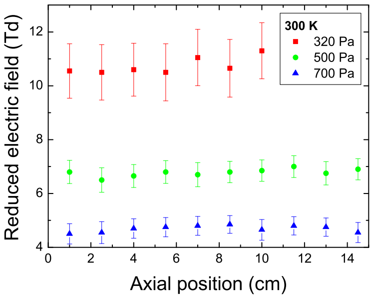

N_2 rotational temperature in $C\,^3\Pi_u$ state

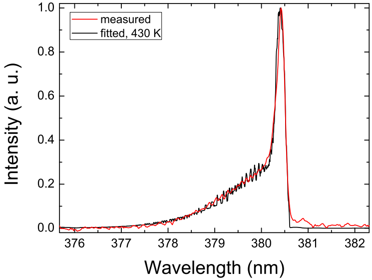

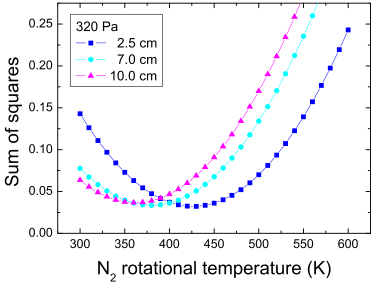

Program Specair. Laux C O 2002. In Fletcher D, Charbonnier J M, Sarma G S R and Magin T, eds., *von Karman Institute Lecture Series 2002–07, Physico-Chemical Modeling of High Enthalpy and Plasma Flows* Rhode-Saint-Gencse, Belgium.

N_2 rotational temperature in $C\,^3\Pi_u$ state

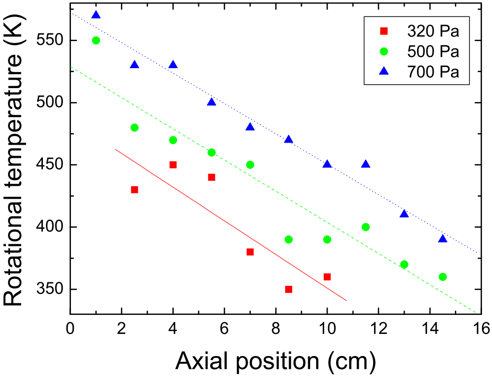

Effect of gas temperature

300 K | N_2 rotational temperature

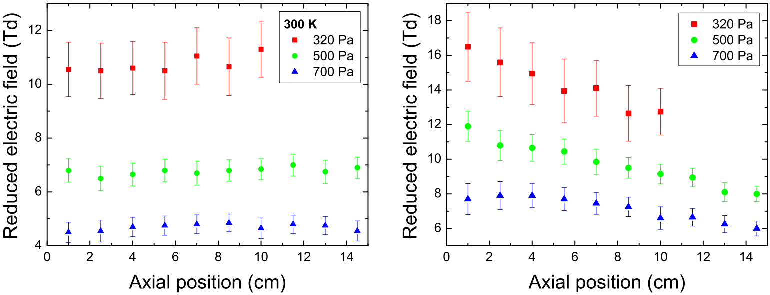

- heating by oscillating field is governed by E/N and ω/N, elastic collisions inhance heating
- ω/N is not constant along the column
- in effective field approximation

$$E_{\text{eff}} = \frac{E_0}{\sqrt{2}} \frac{1}{\sqrt{1+\omega^2/\nu^2}}$$

Self-absorption

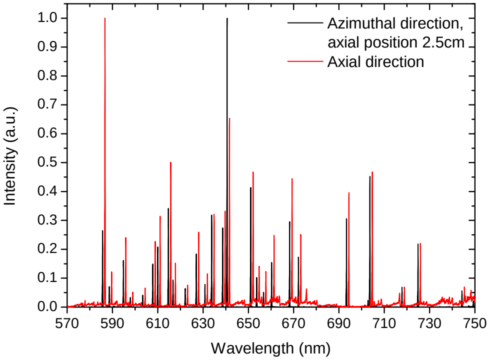

Effective branching fractions Γ_{ij}

- isolated atom

$$\Gamma_{ij} = \frac{A_{ij}}{\sum_l A_{il}}$$

- plasma

$$\Gamma_{ij}^{\mathrm{eff}} = \frac{g(k_{ij}^0 L) A_{ij}}{\sum_l g(k_{il}^0 L) A_{il}}$$

- absorption coefficient

$$k_{ij}^0 = \frac{\lambda_{ij}^3}{8\pi^{3/2}} \sqrt{\frac{m_0}{2k_{\mathrm{b}} T}} \frac{g_i}{g_j} A_{ij} n_j$$

- measured

$$\Gamma_{ij}^{\mathrm{exp}} = \frac{I_{ij}/h\nu_{ij}}{\sum_l I_{il}/h\nu_{il}}$$

Escape factor

- Mewe approximate expression

$$g(k_{ij}^0 L) = \frac{2 - \mathrm{e}^{-k_{ij}^0 L/1000}}{1 + k_{ij}^0 L}$$

- assumption of homogeneous distribution of atoms
- e.g. Ar $2p_6 \rightarrow 1s_5$ (763.5 nm), $\rho = 10\,\mathrm{cm}$

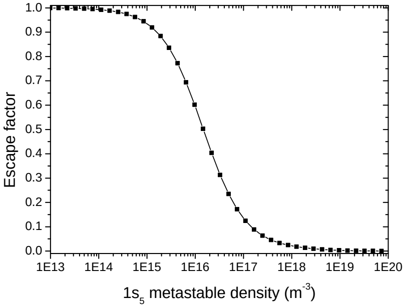

Example – density of Ti and Ti^{+} in magnetron discharge

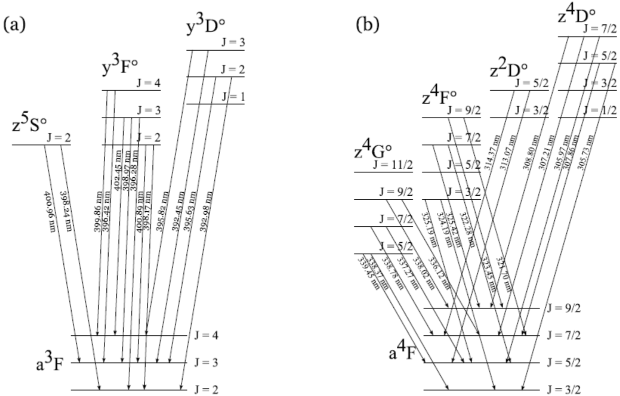

Figure 1. Energy levels and selected transitions for density measurement of (a) Ti neutral atom and (b) Ti ion.

Vašina P 2015 *Plasma Sources Sci. Technol.* **24** 065022

Example – density of Ti and Ti^{+} in magnetron discharge

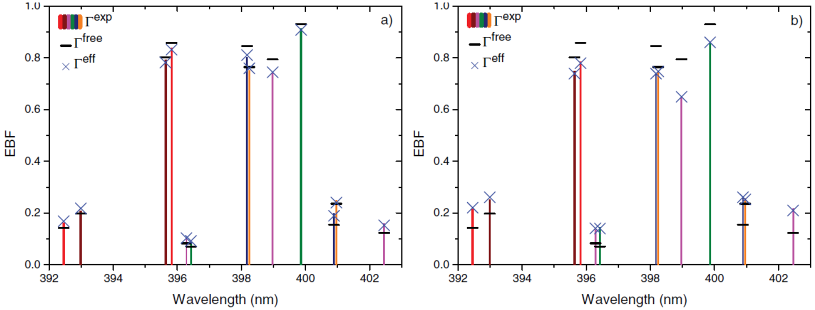

Example – density of Ti and Ti^+ in magnetron discharge

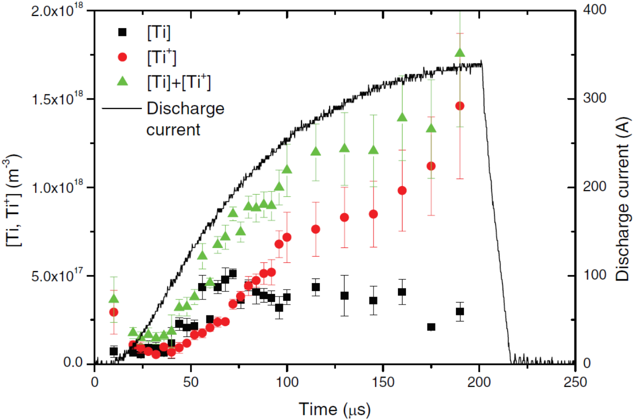

Figure 7. Measurements of the Ti atom and ion density for 200 μs pulse in HiPIMS mode. The pressure was set to 5 Pa, the repetition rate to 20 Hz and the optical fiber was placed 23 mm above the target surface. The total density of the sputtered species is added too.